

Local Intensity Order Transformation for Robust Curvilinear Object Segmentation

Tianyi Shi, Nicolas Boutry, Yongchao Xu, Thierry Géraud

Abstract—Segmentation of curvilinear structure, such as blood vessels in retinal images and cracks in pavement and road images, is important for further image analysis. Currently, deep learning-based methods have achieved impressive performance on curvilinear object segmentation. Yet, most of them mainly focus on finding powerful deep architectures, but ignore to capture the inherent curvilinear structure feature (*i.e.*, curvilinear structure darker than the context) for a more robust representation. In consequence, the performance usually drops a lot on cross-datasets, which poses great challenges in practice. In this paper, we aim to improve the generalizability by introducing a novel local intensity order transformation (LIOT). Specifically, we transfer a gray-scale image into a contrast-invariant four-channel image based on the intensity order between each pixel and its nearby pixels along the four (horizontal and vertical) directions. This results in an image representation that preserves the inherent characteristics of curvilinear structure while being robust to contrast changes. Cross-dataset experimental results on DRIVE, STARE, and CHASDB1 demonstrate that LIOT consistently improves the generalizability of some state-of-the-art methods. Additionally, cross-dataset evaluation between retinal and Crack show that LIOT is able to preserves the inherent characteristics of curvilinear structure, while facing to curvilinear objects with a great gap in appearance.

Index Terms—Curvilinear structures, segmentation, local intensity order, deep learning, generalizability

I. INTRODUCTION

Curvilinear object frequently appears on many applications, such as blood vessels in medical imaging [1], [2] and pavement cracks segmentation [3]. These applications are important for retinal disease screening and road condition evaluation to conduct the necessary road maintenance. Thus, curvilinear object segmentation is common and very important. As compared to general object segmentation, curvilinear object segmentation faces particular challenges [4] because of (1) thin, long, and tortuosity shape, (2) inadequate contrast between curvilinear structure and the surrounding background, (3) uneven background illumination, (4) different curvilinear object segmentation applications with totally various image appearances. To cope with these challenges, classical curvilinear segmentation methods [3], [5]–[14] mainly extract engineered features. The traditional methods usually use the filters or mathematical morphology capture one or more special features from images.

T. Shi is with the School of EIC, Huazhong University of Science and Technology (HUST), Wuhan, 430074, China (E-mail: shitianyi@hust.edu.cn).

N. Boutry and T. Géraud are with Laboratoire de Recherche et Développement de l'EPITA (LRDE), Le Kremlin-Bicêtre, 94276, France (E-mail: {nicolas.boutry, thierry.geraud}@lrde.epita.fr).

Y. Xu is with the School of Computer Science, Wuhan University, Wuhan, 430070, China (E-mail: yongchao.xu@whu.edu.cn).

Corresponding author: Yongchao Xu.

These requires hand-crafted feature and careful parameter tuning, which is difficult to handle a wide variety of complex curvilinear object segmentation.

More recent deep learning methods [15]–[24] have brought significant improvement on curvilinear object segmentation and became the mainstream methods. These methods adapt various network architectures to improve the performance on in-dataset performance. Although achieving high accuracy, these methods require intensive training procedures that results in models may not be easily generalize to other applications where data is not similar. Their performances drop significantly for different datasets or even a little contrast change. Thus, the generalizability to curvilinear objects also remains a bottlenecks for these deep learning-based methods. Currently, most mainstream curvilinear object segmentation methods based on deep learning mainly focus on improve performances in-dataset evaluation. Few of them focus on improving the generalizability to various curvilinear object segmentation. Although each application faces similar task to segment the curvilinear structure, it is difficult to capture these curvilinear structure features for deep learning-based methods explicitly, comparing with the classical methods. Indeed, most existing deep learning-based methods are sensitive to data with various appearances. As shown in Fig. 1, one may achieve good results on images similar to the training dataset. Yet, the segmentation accuracy greatly drops on the same image with changed contrast. Just the change of illumination makes deep learning methods difficult to obtain curvilinear structure. The difference between various applications is a greater gap in appearance. This demonstrates that deep learning-based methods don't really capture the characteristics of curvilinear structure. Therefore, a method to help the deep learning-based methods capture the inherent characteristics of curvilinear structure is really urgent.

In this paper, we aim to address the above issue and focus on improving the generalizability of current deep learning-based methods in segmenting curvilinear object. Instead of directly operating on the original image, we introduce a novel image transformation called *Local Intensity Order Transformation (LIOT)*, which is a generalization representation for curvilinear structure and a invariant to the increasing change of image contrast. Specifically, we compare the intensity order of a given pixel to the values of its nearby neighbors (*e.g.* along the four horizontal and vertical directions within a certain distance). In this way, we transform the original image into a new four-channel one, which does not depend on the absolute intensity value but the relative intensity order to capture the inherent characteristics of curvilinear structure. Such a trans-

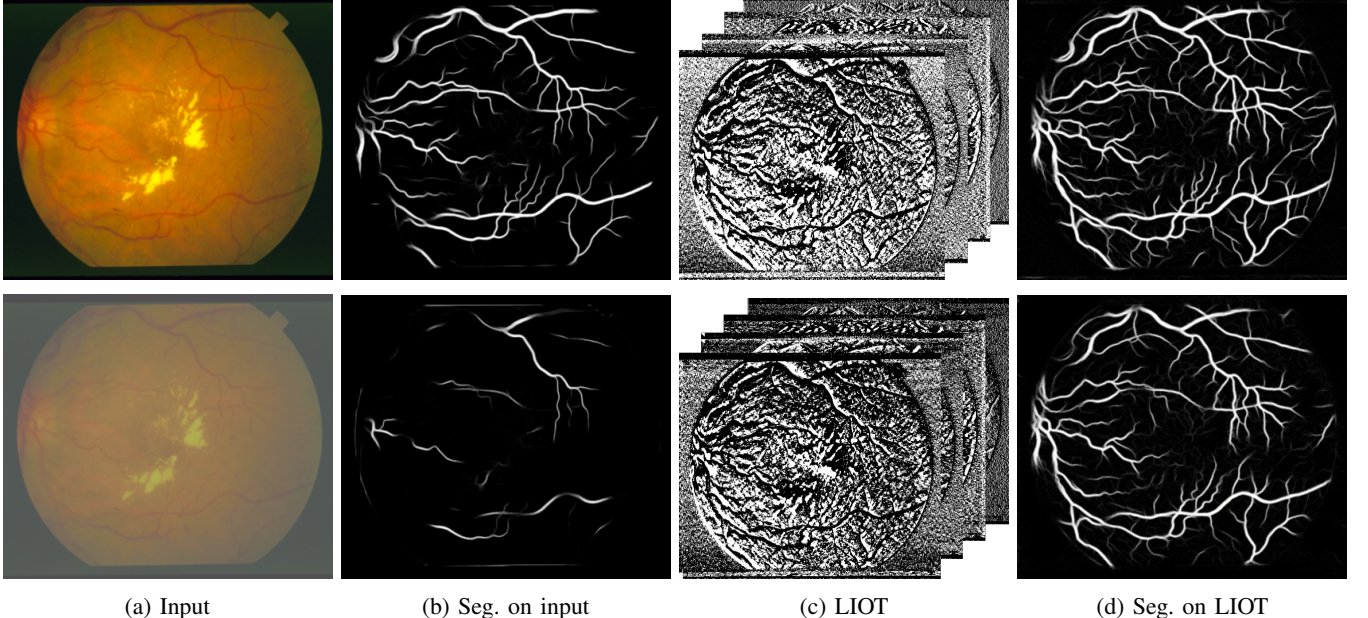


Fig. 1: An example of segmentation results on an image and the same image with changed contrast. Top row: segmentation on the original image by IterNet [25]; Bottom row: segmentation on contrast changed image. Different from direct segmentation on the original image, the proposed LIOT is invariant to contrast changes and thus yields robust segmentation results.

formation also features an interesting characteristic: invariant to the increasing contrast change. An example of LIOT is illustrated in Fig. 1. LIOT is robust to capture the curvilinear characteristics and contrast changes, yielding very similar segmentation results for the original image and the one with a contrast change.

The main characteristic of the proposed LIOT is the robustness to curvilinear characteristics and contrast changes. LIOT simply changes the input and can be plugged into any deep learning-based methods. Since the main goal of this paper is not to develop a powerful pipeline that outperforms all other methods in segmenting curvilinear object, we simply apply LIOT to the recent method IterNet [25] and conduct cross-dataset experiments on four datasets: DRIVE [26], STARE [27], CHASEDB1 [12] and Crack [3]. These cross-dataset experiments demonstrate that the proposed contrast-insensitive LIOT is simple yet effective to help deep learning-based methods to capture the characteristics of the curvilinear structure, and improves the generalizability of existing methods.

The main contributions of this paper are three folds: 1) We propose a novel image transform method which can capture the inherent characteristics of curvilinear structures. These LIOT method makes these original curvilinear object to a generalization expression and invariant to the increasing change of image contrast. 2) The proposed LIOT as input to the deep learning-based method can make deep learning-based model express a better generalization. 3) According to cross-dataset experiments, We find that the curvilinear structure information that LIOT capture is a robust and better representation for various curvilinear object segmentation.

The rest of this paper is organized as follows. We shortly review some related works on curvilinear object segmenta-

tion in Section II. The proposed method is then detailed in Section III, followed by extensive experimental results in Section IV. Finally, we conclude and give some perspectives in Section V.

II. RELATED WORKS

Curvilinear structure has been widely exploited recently. We review some representative classical-based and deep learning-based methods for curvilinear object segmentation in Section II-A first. A review for some image transform is discussed in Section II-B. The comparison of the proposed LIOT with these related works is depicted in Section II-C.

A. Curvilinear Object Segmentation

Curvilinear object segmentation methods can be roughly divided into specifically engineered and deep learning-based methods. Before the era of deep learning, Curvilinear object segmentation pipelines usually are based on different techniques ranging from hand-crafted filter and machine learning approaches. Many traditional methods [5], [11]–[14], [28]–[32] are based on these two algorithms. Most recent methods shift to deep neural networks to learn effective features directly from training data.

Classical-based methods: Classical curvilinear object segmentation methods mainly extract engineered features. For instance, Koller *et al.* [28] introduced a method based on a non-linear combination of linear filters, with an edge-detection approach. Subirats *et al.* [30] detected cracks in pavement using the continuous wavelet transform. Narasimha *et al.* [31] used statistical hypothesis test to discriminate vessels in retinal eye-fundus images. Al-Diri *et al.* [32] segmented vessels in retinal images with a related active contour. Marín *et al.* [11]

utilized a 7-D vector for pixel representation. The orientation analysis of gradient vector fields has been proposed for retinal vessel segmentation in [12]. Ricci *et al.* [13] developed the line operator to construct a feature vector for supervised classification using the support vector machine. Some other typical feature vectors used for retinal vessel segmentation are composed of the pixel intensity and 2D Gabor wavelet transform responses [14]. Fraz *et al.* [29] introduced a shape-based method in which centerlines are detected with a first order derivative of gaussian filter applied in four directions. And an accuracy segmentation method was proposed by graph based representations in [33]. Strisciuglio *et al.* [5] proposed a novel operator for the delineation of curvilinear structures in images. Merveille *et al.* [6] proposed a mixed gradient operator for segmentation task.

Deep learning-based methods: Deep learning-based methods significantly improved the performance of curvilinear object segmentation and learned effective features from training data. For example, the neural network is used for retinal vessel segmentation in [18], which does not depend on the carefully engineered feature. Maninis *et al.* [20] used a unified framework of retinal image analysis that provided both retinal vessel and optic disc segmentation. In [19], Yan *et al.* proposed a joint segment-level and pixel-wise loss for retinal vessel segmentation. Guo *et al.* [21] presented a multi-scale deeply supervised network with short connections, achieving good cross-dataset results. In [22], Jin *et al.* integrated deformable convolution into the U-Net. Cherukuri *et al.* [23] proposed a deep model with regularization under geometric priors. Mosinska *et al.* [15] jointed the segmentation and path classification of curvilinear structures to obtain segmentation and path classification. And they [24] also proposed a topology-aware loss to solve the topological mistakes. Wang *et al.* [16] proposed a curvilinear structure segmentation approach using context-aware spatio-recurrent networks. Lei *et al.* [17] proposed a Channel and Spatial Attention Network (CS-Net) based on U-Net that has proven to be effective to extract curvilinear structures from three biomedical imaging modalities.

B. Census Transform

Census Transform (CT) [34] is a non-parametric local transform, which is defined as an ordered set of comparisons of pixel intensity in a local 3×3 neighborhood. Froba *et al.* [35] proposed a MeanCT to use the mean intensity of the neighborhood to increase robustness. Ambrosch *et al.* [36] proposed a SparseCT to use a subset of pixels within the neighborhood for a larger neighborhoods. Chang *et al.* [37] also proposed a sparse CT Mini-census. Fife *et al.* [38] proposed generalized census transform (GCT) to define a family of masks in a 5×5 neighborhood with different levels of sparsity. Presented at the same time as GCT, the center symmetric CT (CSCT) [39] similarly compares pairs of pixels within the census window. And star census transform (SCT) [40] extends GCT by defining masks of symmetrical sequences of connected edges, of equal length, forming star-shaped scan-patterns around the center. Ahlberg *et al.* [41] proposed a genetic algorithm to find a new and powerful

Census Transform methods. Yu *et al.* [42] just used census transform to calculate the illumination characteristics for tree reconstruction optimization. And Lai *et al.* [43] also used census transform in medical imaging. Ramírez *et al.* [44] applied the census transform operator for audio-sisual emotion recognition, due to its robustness to monotonic changes.

C. Comparison with related works

LIOT Versus Classical-based methods: Classical-based methods rely on engineered features to extract curvilinear structure. These methods require careful parameter tuning, hard to result in a good performance in a wide variety of complex curvilinear object segmentation. The proposed LIOT can leverages the deep learning-based methods strong power, which uses the CNN to learn a more effective features. LIOT can be plugged into any the neural networks to take advantage of deep learning-based methods.

LIOT Versus Deep learning-based methods: Deep learning-based methods are mainly inspired by recent object segmentation pipelines, which have not captured explicit curvilinear structure features. They usually have limited ability on cross-dataset performance because training data with a great gap in appearance. These make models may not be easily transferable to other similar curvilinear object applications. LIOT can help resolve this defect by plugged into any deep learning-based methods. Benefiting from the inherent characteristics that the LIOT captures, LIOT is able to get a better generalization performance in various curvilinear object segmentation for deep learning-based methods.

LIOT Versus Census Transform: Ideally image features for segmentation or other tasks should be depended on the structure of the interesting object. Most census transform methods don't pay particular attention to curvilinear structure. The proposed LIOT captures the curvilinear structure from four directions explicitly, comparing with census transform methods. LIOT also takes a long-range comparison into account, which is a sense describe for curvilinear structure (the curvilinear darker or lighter than the context in a relative range). So it is a robust representation for curvilinear structure. We can see that the LIOT captures a better curvilinear structure.

III. PROPOSED METHODOLOGY

A. Overview

The proposed method relies on the local intensity order to capture the curvilinear structure characteristic for various curvilinear object segmentation. Due to a wide applications range from medical to road maintenance, curvilinear object images are obtained from different application scenarios with various appearance. Indeed, curvilinear objects have entirely different color distribution and background. Such an appearance gap makes it difficult for the algorithm to accurately segment different curvilinear object images. Thus, a general method to improve the generalizability for curvilinear segmentation algorithms is urgently needed.

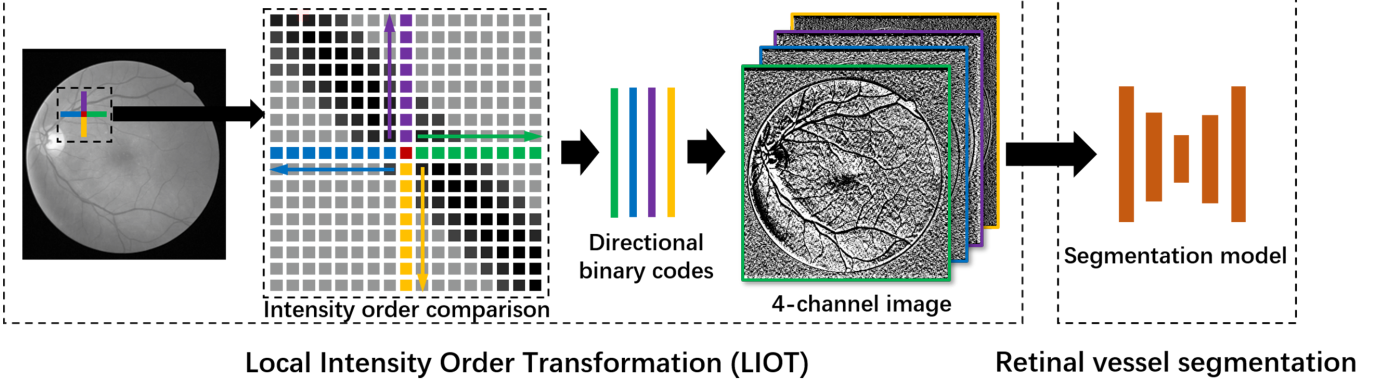


Fig. 2: Overview of the proposed Local Intensity Order Transformation (LIOT) for curvilinear object segmentation. We transform an input image to a 4-channel intensity-order-based image, which is then fed into a segmentation network.

Considering that curvilinear structure usually are darker than the context, we propose to leverage such inherent characteristic which does not depend on the image appearance. Specifically, we introduce a novel image transformation called *Local Intensity Order Transformation* (LIOT) based on the relative intensity order between each pixel and its perpendicular neighbors. Such a transformation does not depend on the absolute value of each pixel, and is thus more robust to contrast changes. Indeed, LIOT is invariant to increasing contrast changes, forming an appropriate image representation for curvilinear object segmentation. Hopefully, LIOT improves the generalizability of curvilinear object segmentation methods. The overall pipeline of the proposed is depicted in Fig. 2.

We first pre-process the image by resizing to a similar scale based on the size of field of view (FOV) and converting the curvilinear image to a gray-scale one. Then we compute LIOT, a 4-direction intensity-order-based transformation, which is then fed into a segmentation network.

B. Image Pre-processing

Images in curvilinear objects may have different image resolutions, and thus have varied widths (in terms of pixels) of curvilinear structure. To cope with such a scale gap, we first resize each image to a similar scale based on the size of field of view (FOV). For Crack dataset, these images don't have the field of view, so we resize the image to a similar scale. Specifically, we rescale the underlying image to a similar scale following the largest diameter of its binary FOV mask. Since the proposed LIOT requires a total order between pixel values, we thus convert the resized color image to a gray-scale one by selecting its green channel.

C. Local Intensity Order Transformation

Though different curvilinear object images may have various contrast and intensity distribution, curvilinear structure are always darker than the context. Based on this property, we propose a novel and robust representation called *Local Intensity Order Transformation* (LIOT) that converts an input gray-scale image into a 4-channel intensity-order-based image. More precisely, as illustrated in Fig. 3, for each pixel p in the

domain Ω of an image f , we compare the value of $f(p)$ with each group of 8 neighboring pixels $\{n_s^i \mid i = 1, \dots, 8\}$ (with distance to p ranging from 1 to 8) lying perpendicular to p , where $s \in \{l, r, t, b\}$ denotes left, right, top, and bottom side of p , respectively. This results in four 2D 8-bit images, where the i -th bit of each converted 2D image f'_s on p corresponds to the binary code given by the order between $f(p)$ and $f(n_s^i)$. These four 2D images of directional binary codes are concatenated together, composing a 4-channel intensity-order-based image $F = [f'_l, f'_r, f'_t, f'_b]$. Formally, for each direction side $s \in \{l, r, t, b\}$, we compute the corresponding image f'_s of directional binary codes on each pixel as follows:

$$f'_s(p) = \sum_{i=1}^8 [f(p) > f(n_s^i)] \times 2^i, \quad (1)$$

where $[f(p) > f(n_s^i)]$ is 1 if the value $f(p)$ is larger than $f(n_s^i)$, otherwise 0.

As depicted in Eq. (1), the proposed transformation is irrespective of absolute intensity values, and only depends on the relative intensity order. LIOT captures the “darker than” property of curvilinear structure and is invariant to increasing change of contrast, which makes LIOT more robust to appearance difference for images from different applications. Therefore, LIOT can improve the generalizability of curvilinear object segmentation methods.

D. Network architecture

Since the major goal is not to develop a powerful network that outperforms other methods, we simply apply LIOT with the recent IterNet [25]. We simply change the input channel to the IterNet [25]. Specifically, The input image is a 4-channels image by LIOT transformation. We change the first convolution layer channel from three to 4-channel for adapting LIOT inputs. And we keep the other structure same as IterNet [25].

E. Training objective

We leverage the network depicted in Section III-D to segment the curvilinear object. The loss is the same as that in

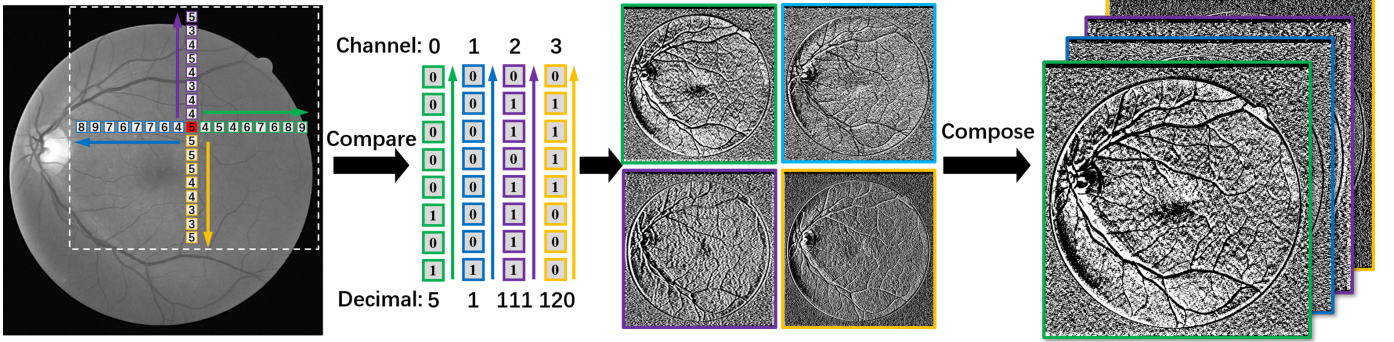


Fig. 3: Illustration of LIOT. For each pixel p , we compare its intensity with the value of every group of 8 neighboring pixels lying perpendicular with p , resulting in a 4-channel image with values in each channel ranging from 0 to 255 (8 bits).

IterNet [25]. The network parameters are optimized with the sigmoid cross entropy loss, defined as:

$$L_i = -y_i \log(p_i) - (1 - y_i) \log(1 - p_i) \quad (2)$$

where y_i represents the binary indicator (0 or 1) whether the label is correct for the pixel i , and p_i is the predicted probability that the pixel i is a foreground pixel.

F. Inference

During testing phase, we convert the original gray-scale image to a 4-channel LIOT image. For each LIOT image, it is contrast-invariant and represents the intensity order between each pixel and its nearby pixels along the four directions. And we use LIOT that represent inherent characteristics of curvilinear structure fed into the network to compute the probability map for segmentation.

IV. EXPERIMENTS

The proposed LIOT is appropriate for improving the generalization of curvilinear object segmentation. In the following, We evaluate the proposed method on four widely adopted datasets: DRIVE [26], STARE [27], and CHASEDB1 [12] and Crack [3]. A short description of these datasets and adopted evaluation protocol is given in Section IV-A. Some implementation details are depicted in Section IV-B. The experimental results of in-dataset evaluation is given in Section IV-C to domonstrate the influence of the proposed LIOT for the original capability of deep learning-based methods. The cross-retinal dataset evaluation, comparing with other methods, is given in Section IV-D. To further demonstrate the generalization ability of LIOT, cross crack and retinal datasets evaluation is given in Section IV-E to demonstrate the generalization ability for difference kind of curvilinear objects. And weakness analysis are given in Section IV-F.

A. Datasets and Evaluation Protocol

DRIVE [26]: The DRIVE dataset consists of 40 color retinal images with a resolution 565×584 , which are split into 20 training images and 20 test images.

STARE [27]: The STARE dataset consists of 20 color retina images divided into 10 training and 10 test images. And each image resolution is 700×605 .

CHASEDB1 [12]: The CHASEDB1 dataset consists of 28 color retinal images with a resolution of 999×960 pixels. We split into 20 training images and 8 test images.

Crack [3]: The Crack dataset contains 206 pavement images with different kinds of crack, which are split into 160 training images and 46 test images. As shown in Fig. 7, the multiple shadows and cluttered background makes their segmentation a challenging task. This dataset mainlt apply to quality inspection and material characterization.

For all experiments, as described in Section III-B, we keep the image size of DRIVE unchanged, and resize the images in STARE, CHASEDB1 and Crack accordingly. Precisely, we resize STARE images from 700×605 to 554×479 and CHASEDB1 images from 999×960 to 584×561 . And we resize the Crack images from 800×600 to 512×512 .

Evaluation protocol: For performance evaluation, we divide the pixels in segmentation results into true positives (TPs), false positives (FPs), false negatives (FNs), and true negatives (TNs). Then, the classical accuracy (Acc), sensitivity (Se), specificity (Sp), area under the receiver operating characteristics curve (AUC), and F1-score are used to evaluate the performance. Besides, we also adopt the connectivity [45] which is a better reflection for curvilinear structural continuity and branching analysis, to further assess the effectiveness of the proposed LIOT.

B. Implementation Details

Data augmentation strategy is adopted to increase the training data and avoid over-fitting. Specifically, images are randomly rotated from -180 to 180 degrees. And images are sheared from -0.1 to 0.1. We also flip images with horizontal and vertical direction. Then, images are shifted from -0.1 to 0.1. Images are randomly zoomed from 0.8 to 1.2. Finally, the augmented images are randomly cropped to 128×128 .

Since the major goal is not to develop a powerful network that outperforms other methods, we simply apply LIOT with the recent IterNet [25]. Following [25], we randomly extract

image patches of size 128×128 and employ a batch size of 32 to train the network using cross-entropy loss for 1000 epochs. And for Crack, the ground truth of Cracks dataset consists of centerlines, so we dilate it by margin of 4 pixels as [24]. We employ a batch size of 32 to train the network using cross-entropy loss for 100 epochs. We adopt Adam [46] with a learning rate of 0.001 to optimize the network. All the experiments are conducted on Tensorflow using a workstation with a single Titan Xp GPU. During inference, overlapping image patches are extracted with a stride equal to 8.

C. In-Dataset Evaluation

The proposed LIOT mainly focus on improving the generalization performance for deep learning-based methods. For this purpose, we first conduct experiments on in-datasets: DRIVE, STARE, CHASEDB1 and Crack to evaluate the influence of LIOT for the ability of model itself. The in-dataset quantitative comparison is depicted in Table I. Compared with baseline method, LIOT perform slightly better on Crack and STARE in terms of Se and F1-score. And the proposed LIOT achieves a close performance in other datasets. We also use the census transform image fed into the network to compare with the proposed LIOT. Specifically, LIOT performs better with Census on all evaluation metrics in average result. Moreover, LIOT achieves competitive or superior performance with Baseline in average result.

This demonstrates that the proposed LIOT will not have a negative effect and slight promotion for deep learning-based methods on in-dataset evaluation. Furthermore, we explore the generalization ability of LIOT in Section IV-D and Section IV-E.

D. Cross-Retinal Dataset Evaluation

We evaluate the proposed LIOT by conducting cross-retina dataset validation between the DRIVE, STARE and CHASEDB1 datasets. We simply replace the original 3-channel color image with the 4-channel LIOT image computed on the green channel.

Some qualitative illustrations are shown in Fig. 4. As depicted in this figure, LIOT is able to correctly segment most retinal vessels, especially those of low contrast. The direct segmentation on the original image fails to retrieve those thin retinal vessels and of low contrast. In particular, as depicted in Fig. 4(b), for the model trained on DRIVE, using LIOT can accurately most retinal vessels, including those (blue pixels in the cropped region on the right side), are of very low contrast and ignored even by the manual annotation. Yet, we can still find cues in the original image and they are indeed retinal vessels. This demonstrates that LIOT is robust to contrast changes. Indeed, as depicted in Fig. 1, the baseline method poorly segments the retinal vessels for the contrast changed image, for which LIOT still performs similarly with the original image. Thus, LIOT can improve the generalizability of some deep learning-based methods in segmenting retinal vessels.

The quantitative evaluation of LIOT is depicted in Table II. Compared with the baseline method of IterNet [25] directly

operating on the original image, LIOT significantly improves or performs on par with the baseline in terms of classical pixel-level metrics: Se, Sp, Acc, AUC, and F1-score. LIOT also performs better in average result, comparing with Baseline and Census input. In particular, LIOT features a high sensitivity regime, which is important in clinical usage. The “false positives” that are retinal vessels of low contrast and ignored by the manual annotation (described above) also degrades a bit the other classical metrics. Theoretically, LIOT may perform slightly better.

It is noteworthy that LIOT not only improves the pixel-level metrics, but also improves the segmentation performance on the vessel network level. Specifically, as shown in Table II, LIOT consistently improves the connectivity of directing segmenting on the original image. This implies that LIOT improves the integrity of the segmentation effect because connectivity assesses the fragmentation degree between the segmentation result and the ground truth. Besides, the connectivity [25], [45], [47] is also an important clue for clinicians to calculate the complexity and density of branching of the retinal vascular tree to measure patient’s condition [48]. Therefore, LIOT is also potentially useful for clinical disease diagnosis.

Though the goal is not to demonstrate that by simply changing the input image by the proposed LIOT on a baseline method can consistently outperform all other methods, as depicted in Table II, the experimental results show that the proposed method is competitive with all other methods in under cross-dataset validation, demonstrating the potential of the proposed LIOT in segmenting retinal vessels for a wide daily clinical usage.

From the qualitative results depicted in Fig. 4 and quantitative results given in Tab. II, the proposed LIOT is able to capture the curvilinear stucture while the contrast and dataset change.

E. Cross Crack and Retinal Datasets Evaluation

As depicted in Section IV-D, We also evaluate the proposed LIOT by conducting cross-dataset validation between the retinal datasets and Crack dataset. We also replace the original 3-channel color image with the 4-channel LIOT image.

The proposed LIOT is appropriate to improve generalization performance for some deep learning-based methods by capturing the inherent characteristics of curvilinear structure. To further demonstrate the generalization ability of the proposed LIOT, we conduct experiments between three retinal datasets above and Crack dataset.

1) Trained on Crack Test to Retinal Datasets: : As shown in Fig. 7, Crack datatset has a great gap with appearance, comparing with retinal images. Some qualitative results are given in Fig. 5. The proposed LIOT correctly segment the curvilinear structre in retinal images. From this figure, we can observe that LIOT preserves the inherent characteristics of curvilinear structure in retinal images. And LIOT is able to segment the curvilinear structure from the various context. Indeed, the baseline method can not capture curvilinear structure. The direct segmentation on the original image fails to retrieve those retinal vessel. More detail, as depicted in Fig. 6,

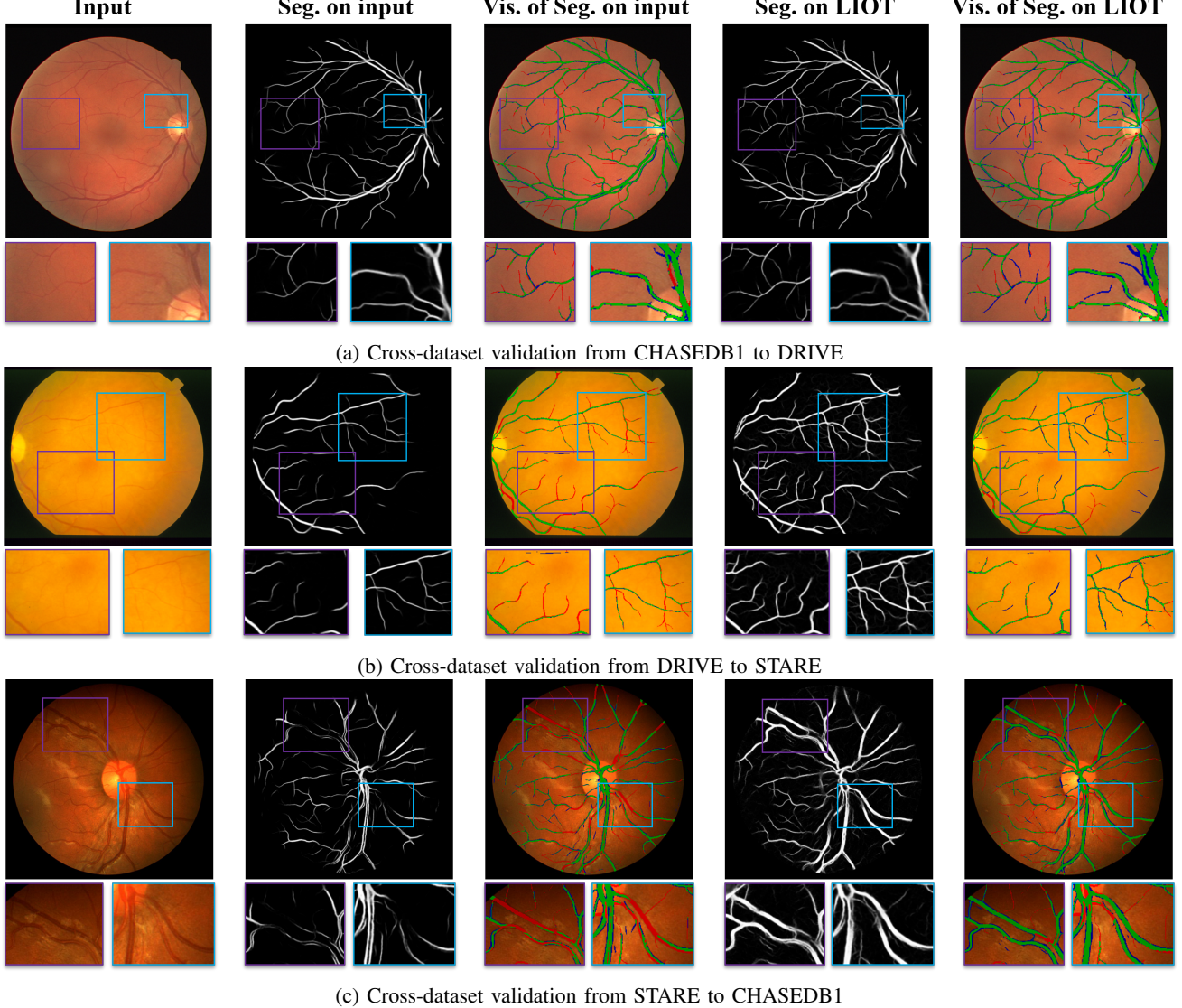


Fig. 4: Visualization of the segmentation results under cross-dataset validation. Green pixels: TPs; Red pixels: FNs; Blue pixels: FPs. Some FPs achieved by LIOT can find evidence in the original image, which might be TPs ignored in the manual annotation.

for the model trained on Crack, using LIOT can accurately capture most retinal vessels, including those blue pixels, are of very low contrast and ignored by the manual annotation. Yet, LIOT can still find these cues in the original image even train on the Crack. This demonstrates that LIOT is robust to contrast changes and has a robust ability to capture the inherent curvilinear structure.

The quantitative results are shown in Tab. III. Compared with baseline method, our proposed method outperforms them by a large margin in terms of Se, AUC and F1-score. The proposed LIOT improves the baseline method range from 34.5% to 41.8% in F1-score, significantly outperforming baseline method. From the quantitative results given in Table IV, the proposed LIOT also makes the gap between retinal and Crack smaller than baseline method observably. Thus, LIOT significantly improves the generalization performs with baseline method. LIOT can help some deep learning-methods to

improve generalization performance, especially for dataset that has curvilinear structure but a great gap with the appearance.

TABLE I: Quantitative In-dataset evaluation of LIOT.

Cross-dataset	Methods	Se	Sp	Acc	AUC	F1
Crack \Rightarrow Crack	Baseline [25]	0.770	0.995	0.991	0.989	0.720
	Census	0.493	0.996	0.989	0.898	0.566
	LIOT	0.777	0.997	0.997	0.985	0.785
DRIVE \Rightarrow DRIVE	Baseline [25]	0.830	0.973	0.955	0.979	0.825
	Census	0.783	0.972	0.948	0.962	0.794
	LIOT	0.816	0.973	0.953	0.975	0.815
STARE \Rightarrow STARE	Baseline [25]	0.792	0.981	0.961	0.972	0.809
	Census	0.763	0.975	0.953	0.964	0.771
	LIOT	0.827	0.975	0.960	0.981	0.810
CHASEDB1 \Rightarrow CHASEDB1	Baseline [25]	0.828	0.979	0.966	0.986	0.813
	Census	0.738	0.979	0.957	0.963	0.756
	LIOT	0.808	0.977	0.962	0.980	0.793
Average	Baseline [25]	0.805	0.982	0.968	0.982	0.792
	Census	0.694	0.980	0.962	0.947	0.722
	LIOT	0.807	0.981	0.968	0.980	0.801

TABLE II: Quantitative cross-dataset evaluation of LIOT and some other methods.

Cross-dataset	Methods	Se	Sp	Acc	AUC	F1	Connectivity
STARE → DRIVE	[49] (2018)	0.671	0.992	0.951	0.975	—	—
	[18] (2015)	0.727	0.981	0.949	0.968	—	—
	[19] (2018)	0.729	0.982	0.949	0.960	—	—
	[23] (2019)	0.772	0.983	0.956	0.977	—	—
	[21] (2019)	0.745	0.978	0.950	0.971	—	—
	Baseline [25]	0.783	0.972	0.947	0.961	0.795	0.774
CHASEDB1 → DRIVE	Census	0.698	0.942	0.911	0.912	0.666	0.662
	LIOT	0.786	0.972	0.947	0.965	0.796	0.775
	[18] (2015)	0.731	0.981	0.948	0.961	—	—
	[21] (2019)	0.696	0.970	0.938	0.952	—	—
CHASEDB1 → STARE	Baseline [25]	0.804	0.973	0.951	0.970	0.810	0.796
	Census	0.720	0.962	0.931	0.936	0.728	0.730
	LIOT	0.808	0.970	0.949	0.970	0.805	0.800
	[18] (2015)	0.703	0.983	0.955	0.967	—	—
	[49] (2018)	0.845	0.973	0.960	0.985	—	—
	[19] (2018)	0.721	0.984	0.957	0.971	—	—
DRIVE → STARE	[23] (2019)	0.778	0.986	0.971	0.982	—	—
	[21] (2019)	0.719	0.982	0.955	0.969	—	—
	Baseline [25]	0.788	0.977	0.958	0.970	0.796	0.778
	Census	0.765	0.974	0.953	0.968	0.771	0.639
CHASEDB1 → STARE	LIOT	0.803	0.974	0.956	0.978	0.793	0.792
	[18] (2015)	0.694	0.983	0.954	0.962	—	—
	[21] (2019)	0.680	0.981	0.950	0.952	—	—
	Baseline [25]	0.727	0.978	0.952	0.958	0.761	0.707
CHASEDB1 → CHASEDB1	Census	0.757	0.971	0.949	0.959	0.755	0.641
	LIOT	0.818	0.972	0.955	0.979	0.794	0.809
	[18] (2015)	0.712	0.979	0.943	0.963	—	—
	[21] (2019)	0.698	0.972	0.944	0.957	—	—
STARE → CHASEDB1	Baseline [25]	0.733	0.968	0.944	0.948	0.728	0.731
	Census	0.682	0.961	0.936	0.943	0.659	0.534
	LIOT	0.798	0.971	0.953	0.975	0.777	0.780
	[18] (2015)	0.724	0.977	0.942	0.955	—	—
CHASEDB1 → CHASEDB1	[21] (2019)	0.673	0.971	0.941	0.951	—	—
	Baseline [25]	0.719	0.961	0.936	0.949	0.697	0.715
	Census	0.572	0.945	0.911	0.879	0.538	0.435
	LIOT	0.772	0.963	0.944	0.964	0.737	0.753
Average	Baseline [25]	0.759	0.972	0.948	0.959	0.765	0.750
	Census	0.699	0.959	0.932	0.934	0.686	0.607
	LIOT	0.798	0.970	0.951	0.972	0.784	0.785

2) *Trained on Retinal Test to Crack Dataset:* : We also evaluate the proposed LIOT on Crack, which is not only a great gap with appearance, but also has multiple shadows in the context. Although these make a challenging task for cross-dataset vailation, the proposed LIOT still segment the curvilinear structure in Crack dataset successfully. As shown in Fig. 7. LIOT is also able to get curvilinear structure with shadow influence in Fig. 7(c). The quantitative comparsion with baseline method on this dataset is given in Tab. III. LIOT also achieves very competitive performance with baseline method. Specifically, LIOT achieves improvement significantly, the baseline method range from 33.6% to 45.4% in F1-score. And LIOT also achieves very competitive results with Baseline and Census in a average result in Tab. III. From the quantitative results given in Table IV, the proposed LIOT also makes the gap between retinal and Crack smaller than baseline method significantly, comparing with Crack or retinal in-dataset F1- score result and cross-dataset result.

From the qualitative results in Fig. 5 and Fig. 7 and quantitative evaluations in Tab. III and Tab. IV, the proposed LIOT is capable to capture the curvilinear structure in various curvilinear object datasets. This demonstrates the generalization ability of the proposed LIOT. LIOT as input can help

TABLE III: Quantitative cross ratinal and crack datasets evaluation of LIOT.

Cross-dataset	Methods	Se	Sp	Acc	AUC	F1
DRIVE⇒Crack	Baseline [25]	0.037	0.997	0.984	0.643	0.061
	Census	0.349	0.995	0.985	0.828	0.408
	LIOT	0.485	0.994	0.987	0.911	0.515
STARE⇒Crack	Baseline [25]	0.022	0.988	0.974	0.371	0.024
	Census	0.040	0.999	0.986	0.696	0.075
	LIOT	0.290	0.995	0.985	0.865	0.360
CHASEDB1⇒Crack	Baseline [25]	0.099	0.994	0.981	0.684	0.129
	Census	0.178	0.998	0.986	0.726	0.272
	LIOT	0.452	0.996	0.988	0.909	0.516
Crack⇒ DRIVE	Baseline [25]	0.131	0.965	0.859	0.646	0.191
	Census	0.532	0.896	0.850	0.812	0.474
	LIOT	0.712	0.895	0.872	0.899	0.585
Crack ⇒ STARE	Baseline [25]	0.130	0.969	0.882	0.626	0.185
	Census	0.436	0.892	0.845	0.750	0.366
	LIOT	0.640	0.911	0.883	0.898	0.530
Crack ⇒ CHASEDB1	Baseline [25]	0.044	0.981	0.897	0.573	0.071
	Census	0.369	0.922	0.872	0.753	0.342
	LIOT	0.650	0.890	0.877	0.895	0.489
Average	Baseline [25]	0.077	0.982	0.930	0.591	0.110
	Census	0.317	0.950	0.921	0.761	0.323
	LIOT	0.538	0.947	0.932	0.896	0.499

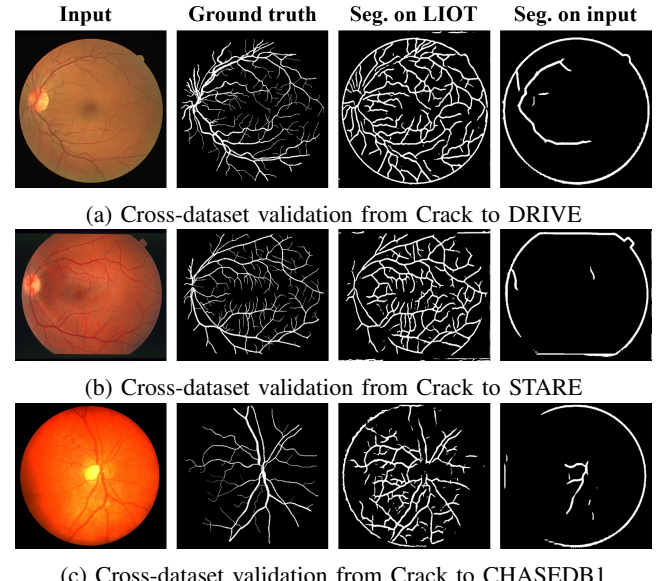


Fig. 5: Visualization of the segmentation results under cross-dataset validation between Crack dataset and retinal datasets.

deep learning-based method express a better generalization in various curvilinear object. And the curvilinear structure information that LIOT capture is a robust and better representation for these various curvilinear objects without considering complex context.

F. Weakness

LIOT also has some limitations. As demonstrated in previous experiments, LIOT performs well in most cases of curvilinear object segmentation applications. It still fails for some situation, such as image with noise, which disturbs the pixel intensity. Since LIOT is based on the intensity order between pairs of pixels, it is sensitive to image noise. In fact, it is reasonable that a generalization and contrast invariant

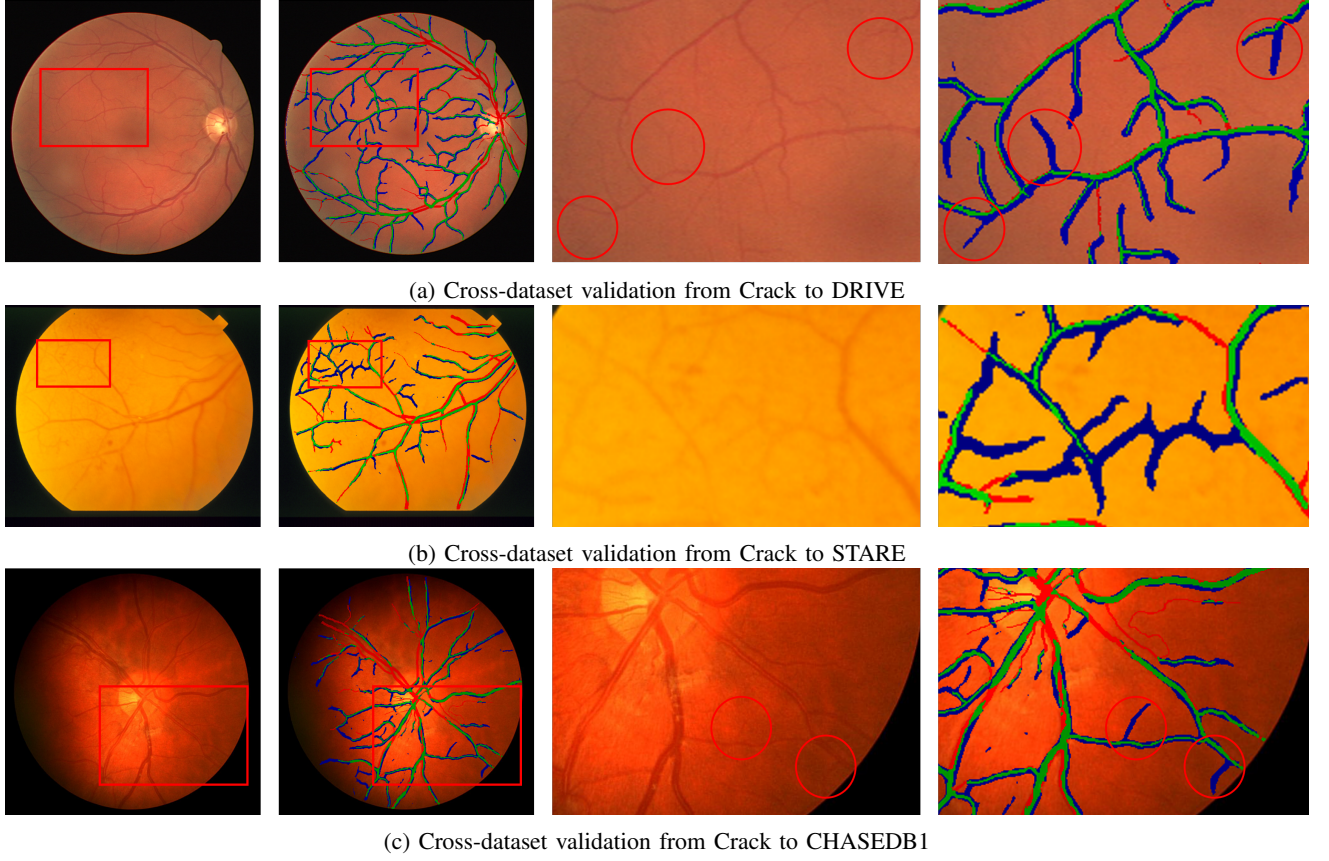


Fig. 6: Visualization of the somd segmentation detail under cross-dataset validation between Crack dataset and retinal datasets. Green pixels: TPs; Red pixels: FNs; Blue pixels: FPs. Some FPs achieved by LIOT can find evidence in the original image, which might be TPs ignored in the manual annotation.

TABLE IV: Quantitative F1-score Gap between in-dataset and cross-dataset results.

Cross-dataset	Methods	Gap	Methods	Gap
Crack \Rightarrow DRIVE	Baseline [25]	0.529	LIOT	0.199
Crack \Rightarrow STARE		0.535		0.255
Crack \Rightarrow CHASEDB1		0.650		0.296
DRIVE \Rightarrow Crack		0.764		0.300
STARE \Rightarrow Crack		0.785		0.450
CHASEDB1 \Rightarrow Crack		0.684		0.277

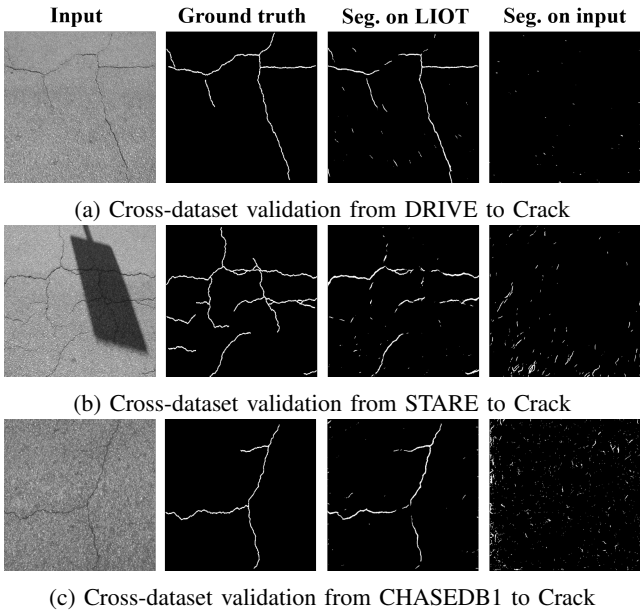


Fig. 7: Visualization of the segmentation results under cross-dataset validation between retinal datasets and Crack dataset.

representation is sensitive to noise. A filtering algorithm (*e.g.*, Gaussian filtering) may alleviate the noise problem. As shown in Fig. 8, we add a gaussian noise to original image and then trans this noise image to LIOT. We also use the Gaussian filter to denoise and trans the denoised image to LIOT. Comparing with these segmentation, the image noise affects the LIOT performance. And a suitable filter to denoise can alleviate the noise affect. In the future, we would like to explore multi-scale LIOT and apply the spirit of LIOT to more curvilinear object segmentation.

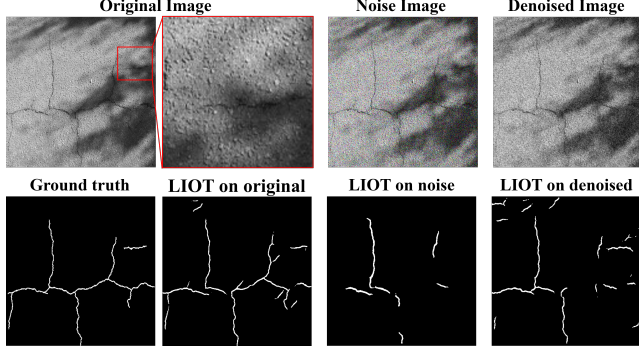


Fig. 8: Visualization of the weakness. Noise affects the segmentation results of LIOT. The influence of noise is solved to a certain extent after denoised.

V. CONCLUSION

In this paper, we aim to improve the generalization ability of the current mainstream deep learning-based curvilinear object segmentation methods. For that, we propose the Local Intensity Order Transformation (LIOT) which converts a gray-scale image to a novel representation which is a generalization representation for curvilinear structure and a invariant to increasing contrast changes. LIOT is built on the intensity order between pairs of pixels, and thus does not depend on the absolute intensity values. Such intensity-order based representation captures the inherent properties of curvilinear objects (curvilinear structure darker than the context). Extensive cross-dataset experiments on three widely adopted retinal vessel segmentation datasets and a Crack dataset demonstrate that the proposed LIOT can consistently improve the classical segmentation pipeline that directly operates on the original image according to capturing the robust curvilinear structure information. Therefore, LIOT forms a simple yet effective way to improve the generalization performance of different models.

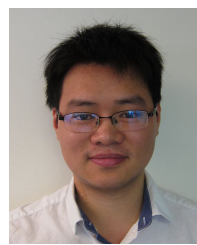
REFERENCES

- [1] M. D. Abràmoff, M. K. Garvin, and M. Sonka, "Retinal imaging and image analysis," *IEEE reviews in biomedical engineering*, vol. 3, pp. 169–208, 2010.
- [2] M. M. Fraz, P. Remagnino, A. Hoppe, B. Uyyanonvara, A. R. Rudnicka, C. G. Owen, and S. A. Barman, "Blood vessel segmentation methodologies in retinal images—a survey," *Computer methods and programs in biomedicine*, vol. 108, no. 1, pp. 407–433, 2012.
- [3] Q. Zou, Y. Cao, Q. Li, Q. Mao, and S. Wang, "Cracktree: Automatic crack detection from pavement images," *Pattern Recognition Letters*, vol. 33, no. 3, pp. 227–238, 2012.
- [4] P. Bibiloni, M. González-Hidalgo, and S. Massanet, "A survey on curvilinear object segmentation in multiple applications," *Pattern Recognition*, vol. 60, pp. 949–970, 2016.
- [5] N. Strisciuglio, G. Azzopardi, and N. Petkov, "Robust inhibition-augmented operator for delineation of curvilinear structures," *IEEE Trans. on Image Processing*, vol. 28, no. 12, pp. 5852–5866, 2019.
- [6] O. Merveille, B. Naegel, H. Talbot, and N. Passat, "n d variational restoration of curvilinear structures with prior-based directional regularization," *IEEE Trans. on Image Processing*, vol. 28, no. 8, pp. 3848–3859, 2019.
- [7] R. Annunziata, A. Kheirkhah, P. Hamrah, and E. Trucco, "Boosting hand-crafted features for curvilinear structure segmentation by learning context filters," in *Proc. of Intl. Conf. on Medical Image Computing and Computer Assisted Intervention*. Springer, 2015, pp. 596–603.
- [8] M. W. Law and A. C. Chung, "Three dimensional curvilinear structure detection using optimally oriented flux," in *Proc. of European Conference on Computer Vision*. Springer, 2008, pp. 368–382.
- [9] D.-S. Huang, W. Jia, and D. Zhang, "Palmpoint verification based on principal lines," *Pattern Recognition*, vol. 41, no. 4, pp. 1316–1328, 2008.
- [10] H. Zhao, J. Kumagai, M. Nakagawa, and R. Shibasaki, "Semi-automatic road extraction from high-resolution satellite image," *International Archives of the Photogrammetry, Remote Sensing and Spatial Information Sciences-ISPRS Archives*, vol. 34, 2002.
- [11] D. Marín, A. Aquino, M. E. Gegúndez-Arias, and J. M. Bravo, "A new supervised method for blood vessel segmentation in retinal images by using gray-level and moment invariants-based features," *IEEE Trans. on Medical Imaging*, vol. 30, no. 1, pp. 146–158, 2010.
- [12] M. M. Fraz, P. Remagnino, A. Hoppe, B. Uyyanonvara, A. R. Rudnicka, C. G. Owen, and S. A. Barman, "An ensemble classification-based approach applied to retinal blood vessel segmentation," *IEEE Transactions on Biomedical Engineering*, vol. 59, no. 9, pp. 2538–2548, 2012.
- [13] E. Ricci and R. Perfetti, "Retinal blood vessel segmentation using line operators and support vector classification," *IEEE Trans. on Medical Imaging*, vol. 26, no. 10, pp. 1357–1365, 2007.
- [14] J. V. Soares, J. J. Leandro, R. M. Cesar, H. F. Jelinek, and M. J. Cree, "Retinal vessel segmentation using the 2-d gabor wavelet and supervised classification," *IEEE Trans. on Medical Imaging*, vol. 25, no. 9, pp. 1214–1222, 2006.
- [15] A. Mosinska, M. Koziński, and P. Fua, "Joint segmentation and path classification of curvilinear structures," *IEEE Trans. Pattern Anal. Mach. Intell.*, vol. 42, no. 6, pp. 1515–1521, 2019.
- [16] F. Wang, Y. Gu, W. Liu, Y. Yu, S. He, and J. Pan, "Context-aware spatio-recurrent curvilinear structure segmentation," in *Proc. of IEEE Intl. Conf. on Computer Vision and Pattern Recognition*, 2019, pp. 12648–12657.
- [17] L. Mou, Y. Zhao, L. Chen, J. Cheng, Z. Gu, H. Hao, H. Qi, Y. Zheng, A. Frangi, and J. Liu, "Cs-net: channel and spatial attention network for curvilinear structure segmentation," in *Proc. of Intl. Conf. on Medical Image Computing and Computer Assisted Intervention*. Springer, 2019, pp. 721–730.
- [18] Q. Li, B. Feng, L. Xie, P. Liang, H. Zhang, and T. Wang, "A cross-modality learning approach for vessel segmentation in retinal images," *IEEE Trans. on Medical Imaging*, vol. 35, no. 1, pp. 109–118, 2015.
- [19] Z. Yan, X. Yang, and K.-T. Cheng, "Joint segment-level and pixel-wise losses for deep learning based retinal vessel segmentation," *IEEE Transactions on Biomedical Engineering*, vol. 65, no. 9, pp. 1912–1923, 2018.
- [20] K.-K. Maninis, J. Pont-Tuset, P. Arbeláez, and L. Van Gool, "Deep retinal image understanding," in *Proc. of Intl. Conf. on Medical Image Computing and Computer Assisted Intervention*. Springer, 2016, pp. 140–148.
- [21] S. Guo, K. Wang, H. Kang, Y. Zhang, Y. Gao, and T. Li, "Bts-dsn: Deeply supervised neural network with short connections for retinal vessel segmentation," *International journal of medical informatics*, vol. 126, pp. 105–113, 2019.
- [22] Q. Jin, Z. Meng, T. D. Pham, Q. Chen, L. Wei, and R. Su, "Dunet: A deformable network for retinal vessel segmentation," *Knowledge-Based Systems*, vol. 178, pp. 149–162, 2019.
- [23] V. Cherukuri, V. K. BG, R. Bala, and V. Monga, "Deep retinal image segmentation with regularization under geometric priors," *IEEE Trans. on Image Processing*, 2019.
- [24] A. Mosinska, P. Marquez-Neila, M. Koziński, and P. Fua, "Beyond the pixel-wise loss for topology-aware delineation," in *Proc. of IEEE Intl. Conf. on Computer Vision and Pattern Recognition*, 2018, pp. 3136–3145.
- [25] L. Li, M. Verma, Y. Nakashima, H. Nagahara, and R. Kawasaki, "Iternet: Retinal image segmentation utilizing structural redundancy in vessel networks," in *Proc. of IEEE Winter Conf. on Applications of Computer Vision*, 2020, pp. 3656–3665.
- [26] J. Staal, M. D. Abràmoff, M. Niemeijer, M. A. Viergever, and B. Van Ginneken, "Ridge-based vessel segmentation in color images of the retina," *IEEE Trans. on Medical Imaging*, vol. 23, no. 4, pp. 501–509, 2004.
- [27] A. Hoover, V. Kouznetsova, and M. Goldbaum, "Locating blood vessels in retinal images by piecewise threshold probing of a matched filter response," *IEEE Trans. on Medical Imaging*, vol. 19, no. 3, pp. 203–210, 2000.
- [28] T. M. Koller, G. Gerig, G. Szekely, and D. Dettwiler, "Multiscale detection of curvilinear structures in 2-d and 3-d image data," in *Proc. of IEEE Intl. Conf. on Computer Vision*. IEEE, 1995, pp. 864–869.

- [29] M. M. Fraz, S. A. Barman, P. Remagnino, A. Hoppe, A. Basit, B. Uyyanonvara, A. R. Rudnicka, and C. G. Owen, "An approach to localize the retinal blood vessels using bit planes and centerline detection," *Computer methods and programs in biomedicine*, vol. 108, no. 2, pp. 600–616, 2012.
- [30] P. Subirats, J. Dumoulin, V. Legeay, and D. Barba, "Automation of pavement surface crack detection using the continuous wavelet transform," in *Proc. of IEEE Intl. Conf. on Image Processing*. IEEE, 2006, pp. 3037–3040.
- [31] H. Narasimha-Iyer, V. Mahadevan, J. M. Beach, and B. Roysam, "Improved detection of the central reflex in retinal vessels using a generalized dual-gaussian model and robust hypothesis testing," *IEEE Transactions on Information Technology in Biomedicine*, vol. 12, no. 3, pp. 406–410, 2008.
- [32] B. Al-Diri, A. Hunter, and D. Steel, "An active contour model for segmenting and measuring retinal vessels," *IEEE Trans. on Medical Imaging*, vol. 28, no. 9, pp. 1488–1497, 2009.
- [33] E. Türetken, F. Benmansour, B. Andres, P. Glowacki, H. Pfister, and P. Fua, "Reconstructing curvilinear networks using path classifiers and integer programming," *IEEE Trans. Pattern Anal. Mach. Intell.*, vol. 38, no. 12, pp. 2515–2530, 2016.
- [34] R. Zabih and J. Woodfill, "A non-parametric approach to visual correspondence," in *IEEE Trans. Pattern Anal. Mach. Intell.* Citeseer, 1996.
- [35] B. Froba and A. Ernst, "Face detection with the modified census transform," in *Sixth IEEE International Conference on Automatic Face and Gesture Recognition, 2004. Proceedings*. IEEE, 2004, pp. 91–96.
- [36] K. Ambrosch, C. Zinner, and H. Leopold, "A miniature embedded stereo vision system for automotive applications," in *2010 IEEE 26th Convention of Electrical and Electronics Engineers in Israel*. IEEE, 2010, pp. 000 786–000 789.
- [37] N. Y.-C. Chang, T.-H. Tsai, B.-H. Hsu, Y.-C. Chen, and T.-S. Chang, "Algorithm and architecture of disparity estimation with mini-census adaptive support weight," *IEEE Transactions on Circuits and Systems for Video Technology*, vol. 20, no. 6, pp. 792–805, 2010.
- [38] W. S. Fife and J. K. Archibald, "Improved census transforms for resource-optimized stereo vision," *IEEE Transactions on Circuits and Systems for Video Technology*, vol. 23, no. 1, pp. 60–73, 2012.
- [39] R. Spangenberg, T. Langner, and R. Rojas, "Weighted semi-global matching and center-symmetric census transform for robust driver assistance," in *International Conference on Computer Analysis of Images and Patterns*. Springer, 2013, pp. 34–41.
- [40] J. Lee, D. Jun, C. Eem, and H. Hong, "Improved census transform for noise robust stereo matching," *Optical Engineering*, vol. 55, no. 6, p. 063107, 2016.
- [41] C. Ahlberg, M. L. Ortiz, F. Ekstrand, and M. Ekstrom, "Unbounded sparse census transform using genetic algorithm," in *Proc. of IEEE Winter Conf. on Applications of Computer Vision*. IEEE, 2019, pp. 1616–1625.
- [42] S. Yu, Y. He, Z. Chen, C. Ru, and M. Pang, "Stereo matching method based on combination characteristic cost computing and unstable tree reconstruction optimization and its application in medical images," *Journal of Medical Imaging and Health Informatics*, vol. 10, no. 3, pp. 646–653, 2020.
- [43] X. Lai, X. Xu, J. Zhang, Y. Fang, and Z. Huang, "An efficient implementation of a census-based stereo matching and its applications in medical imaging," *Journal of Medical Imaging and Health Informatics*, vol. 9, no. 6, pp. 1152–1159, 2019.
- [44] J. Y. R. Cornejo and H. Pedrini, "Audio-visual emotion recognition using a hybrid deep convolutional neural network based on census transform," in *2019 IEEE International Conference on Systems, Man and Cybernetics (SMC)*. IEEE, 2019, pp. 3396–3402.
- [45] M. E. Gegúndez-Arias, A. Aquino, J. M. Bravo, and D. Marín, "A function for quality evaluation of retinal vessel segmentations," *IEEE Trans. on Medical Imaging*, vol. 31, no. 2, pp. 231–239, 2011.
- [46] D. P. Kingma and J. Ba, "Adam: A method for stochastic optimization," *arXiv preprint arXiv:1412.6980*, 2014.
- [47] S. Moccia, E. De Momi, S. El Hadji, and L. S. Mattos, "Blood vessel segmentation algorithms—review of methods, datasets and evaluation metrics," *Computer methods and programs in biomedicine*, vol. 158, pp. 71–91, 2018.
- [48] T. L. Torp, R. Kawasaki, T. Y. Wong, T. Peto, and J. Grauslund, "Temporal changes in retinal vascular parameters associated with successful panretinal photocoagulation in proliferative diabetic retinopathy: a prospective clinical interventional study," *Acta ophthalmologica*, vol. 96, no. 4, pp. 405–410, 2018.
- [49] A. Oliveira, S. Pereira, and C. A. Silva, "Retinal vessel segmentation based on fully convolutional neural networks," *Expert Systems with Applications*, vol. 112, pp. 229–242, 2018.



Tianyi Shi received the B.S. degree from the School of Materials Science and Engineering, Huazhong University of Science and Technology (HUST), Wuhan, China, in 2017, where he is currently pursuing the PhD's degree. His main research interests include image segmentation, medical image analysis and deep learning.



Yongchao Xu received in 2010 both the engineer degree in electronics & embedded systems at Polytech Paris Sud and the master degree in signal processing & image processing at Université Paris Sud, and the Ph.D. degree in image processing and mathematical morphology at Université Paris Est in 2013. He is currently a Professor with the School of Computer Science, Wuhan University. His research interests include mathematical morphology, image segmentation, medical image analysis, and deep learning.